

Photovoltaic effect in bent quantum wires

Yuriy V. Pershin* and Carlo Piermarocchi

Department of Physics and Astronomy, Michigan State University, East Lansing, Michigan 48824-2320, USA

We propose a scheme for the generation of photocurrent in bent quantum wires. We calculate the current using a generalized Landauer-Büttiker approach that takes into account the electromagnetic radiation. For circularly polarized light, we find that the curvature in the bent wire induces an asymmetry in the scattering coefficients for left and right moving electrons. This asymmetry results in a current at zero bias voltage. The effect is due to the geometry of the wire which transforms the photon angular momentum into translational motion for the electrons.

PACS numbers: 73.21.Hb, 72.40.+w, 72.30.+q

Recently many schemes for photocurrent generation in confined electron systems have been investigated.^{1–18} In particular, mechanisms of photocurrent generation by circularly polarized radiation have been considered in quantum rings^{15,17} and helical quantum wires.¹⁶ These geometries are particularly interesting because they can transform angular momentum (from the photon circular polarization) to translational motion (electron current).¹⁵ The experimental realization of these schemes has not yet been reported. In fact, the detection of the photocurrent in isolated quantum rings is experimentally challenging and helical quantum wires cannot be fabricated using standard growth techniques.

In this paper, we consider the photocurrent induced in ballistic quantum wires bent as in Fig. 1. Quantum wires of this geometry can be easily fabricated using standard semiconductor growth techniques, like for instance V-grooving.¹⁹ The setup in Fig. 1 can also be realized by bending a single carbon nanotube on a surface. Using a scattering theory approach we show that the photocurrent can be strong in this geometry. In a GaAs based quantum wire under a radiation of 33mW/cm² we obtain a current of the order of 10 pA, which is measurable with standard methods. The circularly polarized radiation propagating perpendicularly to the wire plane induces on the electrons in the curved region a sliding potential of the form $V(s/R \pm \omega t)$, where s is the position in the wire, R is the radius of curvature, and $\hbar\omega$ is the radiation energy. This sliding potential is an asymmetric scattering potential for left and right moving electrons, and the difference in the transmission probabilities results in a steady current. The classical interpretation of the effect is that only the electrons moving in the same direction of the sliding potential are accelerated. We found that quantum interference plays an important role in the current. In fact, the energy dependence of the current shows not only a peak at the Fermi energy, expected from a classical picture, but also several additional peaks. These additional peaks are due to the quantum interference of transmitted and reflected waves at the points where the curvature of the wire changes.

As shown in Fig. 1, we model the curved quantum wire in the (x, y) plane using two straight quantum wires (regions 1 and 3) connected by an arc of a radius R (region

2). On the opposite side the straight quantum wires are connected to the left (L) and right (R) electron reservoirs. The arc length is given by $L = \varphi R$, where φ is the arc angle. We assume that a circularly polarized electromagnetic radiation propagates in the z direction, perpendicular to (x, y) plane. Experimentally, an electromagnetic cavity can be used to confine the radiation only in the bent segment of the wire. The electromagnetic cavity will also enhance the radiation-electron coupling and increase the current. In any case, a radiation acting on the straight segments of the wire will not generate a current alone, no matter what polarization is used. We will therefore neglect the effect of the radiation on the straight segments. The electron motion along the curved wire is one-dimensional and we define a parameter s which indicates the position along the wire. For simplicity, let us select the point $s = 0$ at the contact of regions 1 and 2. The single electron Hamiltonian in the effective-mass approximation is given by

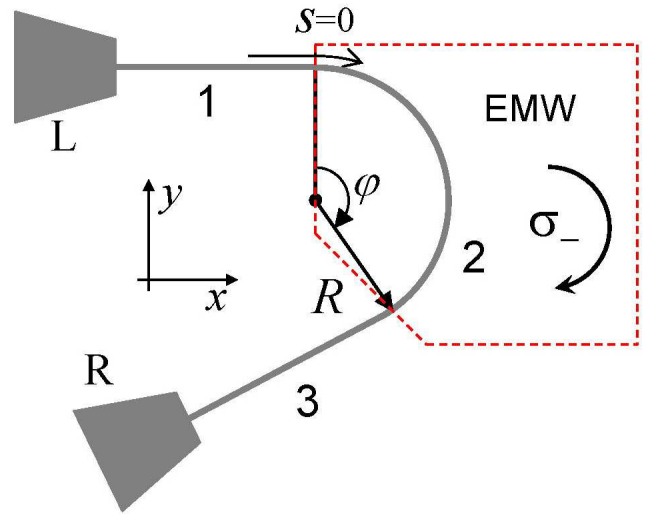


FIG. 1: (Color online) Curved quantum wire irradiated by a circularly polarized electromagnetic wave (EMW) with the electric field component precessing in (x, y) -plane.

$$H = -\frac{\hbar^2}{2m^*} \frac{\partial^2}{\partial s^2} + (\theta(s) - \theta(s-L))[-\mathbf{d}\mathbf{E} - U_g], \quad (1)$$

where m^* is the effective mass, $\theta(\dots)$ is the step function, and $\mathbf{d} = -e\mathbf{r}$ is the dipole moment. The electric field in the radiation is written as $\mathbf{E} = E_0 \cos(\omega t)\hat{x} \pm E_0 \sin(\omega t)\hat{y}$, where E_0 and ω are the electric field amplitude and frequency, \hat{x} and \hat{y} are unit vectors in the x and y directions, and \pm corresponds to a σ_{\pm} circular polarization. The first term in Eq. (1) is the kinetic energy, the second term is the dipolar interaction with the radiation and the third term is the geometrical potential $U_g = \hbar^2/(8m^*R^2)$ which describes the effect of the curvature.^{23,24} The factor $(\theta(s) - \theta(s-L))$ makes the second and third terms different than zero only in the bent segment (region 2). Moreover, we assume that the curved quantum wire is narrow in the transverse directions, so that our model is limited only to transitions within the lowest transverse subband.

Using the substitution $y = R \cos(s/R)$ and $x = R \sin(s/R)$, we can rewrite the interaction term in Eq. (1) as

$$-\mathbf{d}\mathbf{E} = 2eRE_0 \sin\left(\frac{s}{R} \pm \omega t\right). \quad (2)$$

According to Eq. (2), the electrons in the constant curvature segment are subjected to a potential that moves forward or backward depending on the helicity of the circularly polarized light. A similar sliding potential describes the interaction of electrons confined by a traveling acoustic wave.²⁰ In our case, the effective wavelength of the confined travelling wave is $2\pi R^{-1}$.

We can write the electric current from the left (L) to the right (R) reservoirs using a generalization^{5,20,21} of the Landauer-Büttiker formula²² that takes into account the radiation

$$I = \frac{2e}{h} \sum_n \int_0^\infty [T_{R,L}(E + n\hbar\omega, E)f_{\mu_L} - T_{L,R}(E + n\hbar\omega, E)f_{\mu_R}] dE. \quad (3)$$

Here e is the electron charge and $T_{R,L}(E + n\hbar\omega, E)$ is the probability that an electron of energy E in the left reservoir is transmitted to the right reservoir in a state of energy $E + n\hbar\omega$. Since we are going to study the current in the absence of external bias, i.e., at $\mu_L = \mu_R = \mu$, Eq. (3) can be rewritten as

$$I = \frac{2e}{h} \int_0^\infty \Delta T(E) f_\mu dE, \quad (4)$$

where

$$\Delta T(E) = \sum_n [T_{R,L}(E + n\hbar\omega, E) - T_{L,R}(E + n\hbar\omega, E)]. \quad (5)$$

We first consider the time-dependent Schrödinger equation in region 2. Taking into account only single

photon absorption and emission processes, corresponding to $n = -1, 0, 1$ in Eq. (5), we write the electronic wave function in the form

$$\psi_2(s, t) = \sum_{n=-1}^1 f_n(s) e^{-\frac{i(E+n\hbar\omega)t}{\hbar}}. \quad (6)$$

In what follows we consider the case of σ_- polarization, as shown in Fig. 1. The σ_+ case is analogous. Substituting (6) into the time-dependent Schrödinger equation and neglecting the terms related to multi-photon absorption and emission, we obtain

$$(E - \hbar\omega + U_g)f_{-1} + \frac{\hbar^2}{2m^*}f_{-1}'' = ieE_0R e^{-i\frac{s}{R}}f_0, \quad (7)$$

$$(E + U_g)f_0 + \frac{\hbar^2}{2m^*}f_0'' = ieE_0R (e^{-i\frac{s}{R}}f_1 - e^{i\frac{s}{R}}f_{-1}), \quad (8)$$

$$(E + \hbar\omega + U_g)f_1 + \frac{\hbar^2}{2m^*}f_1'' = -ieE_0R e^{i\frac{s}{R}}f_0. \quad (9)$$

By looking for solutions of the Eqs. (7-9) in the form $f_{-1} = C_{-1}e^{i(\tilde{k}-\frac{1}{R})s}$, $f_0 = C_0e^{i\tilde{k}s}$, and $f_1 = C_1e^{i(\tilde{k}+\frac{1}{R})s}$, we obtain for the coefficients the system of equations

$$(E - \hbar\omega + U_g)C_{-1} - \frac{\hbar^2\left(\tilde{k} - \frac{1}{R}\right)^2}{2m^*}C_{-1} - ieE_0RC_0 = 0, \quad (10)$$

$$(E + U_g)C_0 - \frac{\hbar^2\tilde{k}^2}{2m^*}C_0 + ieE_0R(C_{-1} - C_1) = 0, \quad (11)$$

$$(E + \hbar\omega + U_g)C_1 + \frac{\hbar^2\left(\tilde{k} + \frac{1}{R}\right)^2}{2m^*}C_1 + ieE_0RC_0 = 0. \quad (12)$$

From the condition that the matrix in the linear system of Eqs. (10-12) has the determinant equal to zero, we obtain the six possible values of \tilde{k} . Therefore, the wave function in the second region is given by

$$\psi_2(s, t) = \sum_{j=1}^6 \sum_{n=-1}^1 C_{n,j} e^{i(\tilde{k}_j + n\frac{1}{R})s} e^{-\frac{i(E+n\hbar\omega)t}{\hbar}}. \quad (13)$$

where the coefficients $C_{-1,j}$ and $C_{1,j}$ can be expressed through $C_{0,j}$ using Eqs. (10) and (12).

In order to find the transmission probability $T_{L,R}$, we solve a scattering problem selecting the wave functions in the 1-st and 3-rd regions as

$$\psi_1(s, t) = e^{ik_0s} e^{-\frac{iEt}{\hbar}} + \sum_{n=-1}^1 r_n e^{-ik_ns} e^{-\frac{i(E+n\hbar\omega)t}{\hbar}}, \quad (14)$$

and

$$\psi_3(s, t) = \sum_{n=-1}^1 t_n e^{ik_ns} e^{-\frac{i(E+n\hbar\omega)t}{\hbar}}, \quad (15)$$

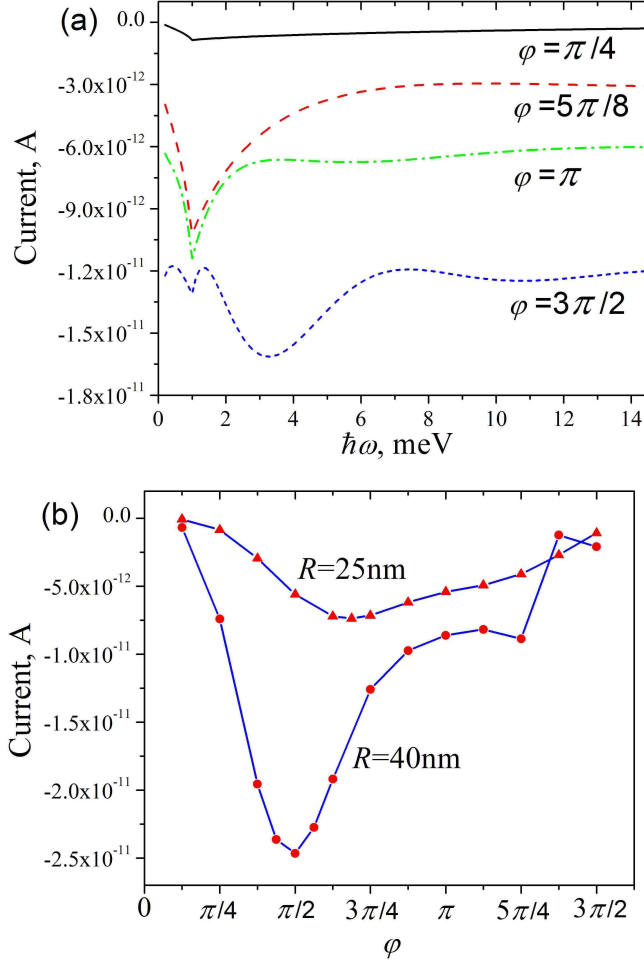


FIG. 2: (Color online) (a) Photocurrent as a function of the photon energy calculated for quantum wires having different arc lengths and $R = 25$ nm. (b) Photocurrent as a function of the arc length at $\hbar\omega = 1$ meV. These plots have been obtained using $E_0 = 500$ V/m, $\mu = 1$ meV, $T = 10$ mK, and $m^* = 0.067m_e$. The electric field amplitude $E_0 = 500$ V/m corresponds to 33 mW/cm² radiation power. All the curves other than $\varphi = \pi/4$ in Fig. 2 (a) have been vertically shifted by steps of $0.3 \cdot 10^{-11}$ A.

where $k_n = \sqrt{2m^*(E + n\hbar\omega)/\hbar^2}$, r_n and t_n are reflection and transmission coefficients, respectively. Matching the wave functions and their derivatives at the boundaries $s = 0$ and $s = L$, we obtain 12 linear equations for the coefficients r_n , t_n and $C_{0,j}$ with $n = -1, 0, 1$ and $j = 1, \dots, 6$. These equations were solved numerically, and the total transmission coefficient from the left to the right reservoir at the energy E was calculated as

$$\sum_{n=-1}^1 T_{R,L}(E + n\hbar\omega, E) = |t_0|^2 + \frac{k_1}{k_0} |t_1|^2 + \theta(E - \hbar\omega) \frac{k_{-1}}{k_0} |t_{-1}|^2. \quad (16)$$

Using a similar scheme, we obtained the total transmis-

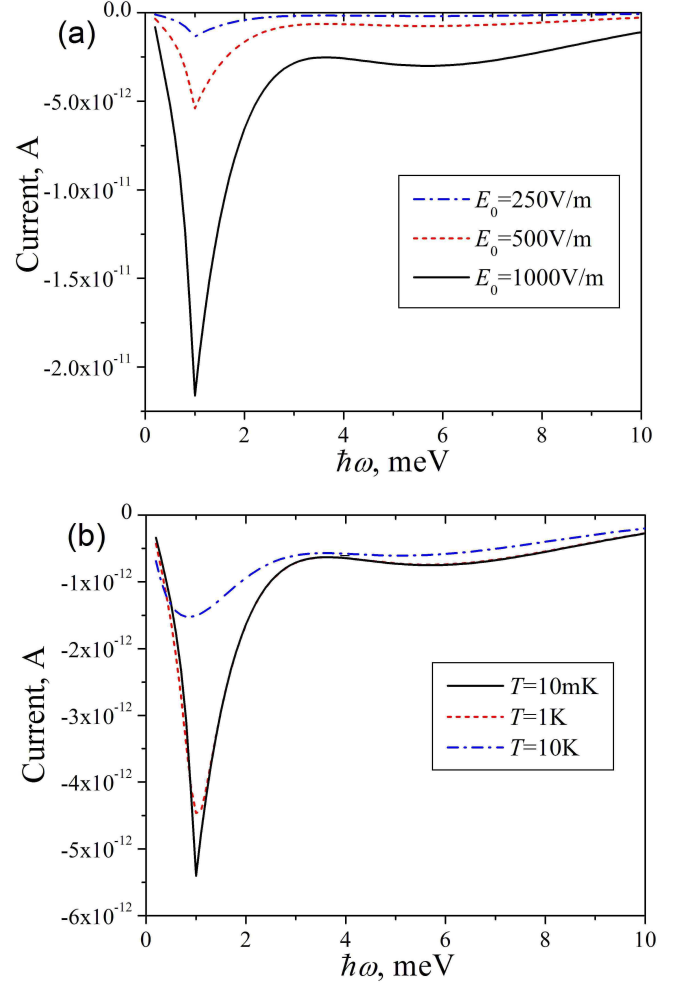


FIG. 3: (Color online) Photocurrent as a function of the photon energy calculated (a) for different radiation intensities at $T = 10$ mK and (b) for different temperatures at $E_0 = 500$ V/m. The other parameters values are as in Fig. 2 with $\varphi = \pi$ and $R = 25$ nm.

sion coefficient in the opposite direction and calculated the current using Eq. (4).

The results of our calculations are shown in Fig. 2 and Fig. 3. Typically, the photocurrent is negative, in agreement with the picture that the potential sliding to the right (for σ_- polarization) increases the transmission probability for right-moving electrons, which results in a negative current because of the negative electron charge e . However, it should be noted that the current can be positive for small values of $\hbar\omega$, as in the $\varphi = 3\pi/2$ curve in Fig. 2(a) (Note that this curve has been shifted vertically by $1.2 \cdot 10^{-11}$ A). This behavior is due to quantum interference phenomena in the reflection and transmission of the electrons across the three regions. As illustrated in Fig. 2(a), the length of the irradiated region has a significant effect on the photocurrent. In quantum wires with a shorter arc, the current as a function of the photon energy is characterized by a single peak at

$\hbar\omega = \mu$. By increasing the arc angle φ additional peaks appears and the peak at $\hbar\omega = \mu$ decreases. We found that the position of these additional peaks is determined only by the arc length (at a fixed R) and does not depend on the radiation intensity. Fig. 2(b) demonstrates that the current at $\hbar\omega = \mu$ is stronger in the wires with larger R and its maximum shifts to smaller φ with increase of R .

The effects of the radiation intensity and finite temperature on the photocurrent are shown in Fig. 3. In Fig. 3(a) we see that the energy dependence of the photocurrent scales with the radiation intensity without changing considerably in shape. The finite temperature (Fig. 3(b)) smoothes the peak at $\hbar\omega = \mu$ and shifts it to lower energy. However, this effect becomes significant only at $T \sim 10\text{K}$, implying that very strict temperature requirements are not needed in the experiment.

In summary, we have demonstrated that circularly polarized electromagnetic radiation induces a current in curved ballistic quantum wires (photovoltaic effect). The current was calculated as a function of the photon energy and length of the bent segment. We have investigated the temperature and intensity dependence of the photocurrent. We found that for a realistic set of parameters a current of the order of 10pA can be observed. In curved quantum wires with a short curved segment, the current dependence on photon energy shows a single peak at the Fermi energy. Larger segments give rise to additional peaks due to the wave reflection and transmission at different region boundaries.

We thank Prof. M. Dykman for many fruitful discussions. This research was supported by the National Science Foundation, Grant NSF DMR-0312491.

-
- * Electronic address: pershin@pa.msu.edu
- ¹ F. Hekking, Yu. V. Nazarov, Phys. Rev. B **44**, 11506 (1991).
 - ² S. Feng, Q. Hu, Phys. Rev. B **48**, 5354 (1993).
 - ³ L. Fedichkin, V. Ryzhii and V. Vyurkov, J. Phys.: Cond. Matter **5**, 6091 (1993).
 - ⁴ A. Grincwajg, L. Y. Gorelik, V. Z. Kleiner, and R. I. Shekhter, Phys. Rev. B **52**, 12 168 (1995).
 - ⁵ F. A. Maaø and L. Y. Gorelik, Phys. Rev. B **53**, 15885 (1996).
 - ⁶ C. S. Tang and C. S. Chu Phys. Rev. B **53**, 4838 (1996).
 - ⁷ S. Blom, L. Y. Gorelik, M. Jonson, R. I. Shekhter, A. G. Scherbakov, E. N. Bogachek, and U. Landman, Phys. Rev. B **58**, 16 305 (1998).
 - ⁸ Y. Levinson and P. Wölfle, Phys. Rev. Lett. **83**, 1399 (1999).
 - ⁹ C. Niu and D. L. Lin, Phys. Rev. B **62**, 4578 (2000).
 - ¹⁰ S. Blom and L. Y. Gorelik, Phys. Rev. B **64**, 045320 (2001).
 - ¹¹ G. Platero and R. Aguado, Phys. Rep. **395**, 1 (2004).
 - ¹² N. G. Galkin, V. A. Margulis, and A. V. Shorokhov, Phys. Rev. B **69**, 113312 (2004).
 - ¹³ Yu. V. Pershin and C. Piermarocchi, Appl. Phys. Lett. **86**, 212107 (2005).
 - ¹⁴ A. Fedorov, Yu. V. Pershin and C. Piermarocchi, cond-mat/0507461.
 - ¹⁵ L. I. Magarill and M. V. Éntin, JETP Lett. **78**, 213 (2003).
 - ¹⁶ L. I. Magarill and A. V. Chaplik, Pis'ma Zh. Eksp. Teor. Fiz. **70**, 607 (1999) [JETP Lett. **70**, 615 (1999)].
 - ¹⁷ Yu. V. Pershin and C. Piermarocchi, cond-mat/0502001.
 - ¹⁸ H. Kosaka, D.S. Rao, H.D. Robinson, P. Bandaru, T. Sakamoto, and E. Yablonovitch, Phys. Rev. B **65**, 201307(R) (2002).
 - ¹⁹ E. Kapon, D. M. Hwang, and R. Bhat, Phys. Rev. Lett. **63**, 430 (1989).
 - ²⁰ F. A. Maaø and Y. Galperin, Phys. Rev. B **56**, 4028 (1997).
 - ²¹ S. Datta and M. P. Anantram, Phys. Rev. B **45**, R13761 (1992).
 - ²² R. Landauer, IBM J. Res. Dev. **1**, 223 (1957); M. Buttiker, Phys. Rev. Lett. **57**, 1761 (1986).
 - ²³ R. C. T. da Costa, Phys. Rev. A **23**, 1982 (1981).
 - ²⁴ S. N. Shevchenko and Yu. A. Kolesnichenko, JETP **92**, 811 (2001).